

Automated Design of Pseudo-Orbiter Phases for Ocean World's Global Mapping

Jose Carlos García Mateas⁽¹⁾, Andrea Bellome⁽¹⁾, Joan-Pau Sánchez Cuartielles⁽¹⁾

⁽¹⁾ ISAE-SUPAERO

Toulouse, France

jose-carlos.garcia-mateas@isae-supero.fr

andrea.bellome2@isae-supero.fr

joan-pau.sanchez@isae-supero.fr

Abstract – This paper presents a two-step automated approach to design pseudo-orbiter phases for the moons of the Outer Planets. The process first discretizes the search space in terms of time-independent nodes and constructs the associated graph adjacency matrix. Subsequently, an exploration is carried out using a deterministic breadth-first algorithm, which traverses the graph and constructs the trajectories. In contrast to existing approaches, the process is completely automated and solves the corresponding constraint satisfaction problem (CSP), providing mission designers with a large catalogue of trajectory options in a short computation time.

I. INTRODUCTION

During the 1970's and early 1980's, the Pioneer and Voyager missions experienced close encounters with the giant planets, revealing the intricacy of such systems [1] [2]. As a result of these first discoveries and the consequent quest of the scientific community for their exploration, dedicated missions such as Galileo and Cassini-Huygens were developed, targeting Jupiter and Saturn respectively, and unveiling the existence of oceans below the surface of Europa, Ganymede, Enceladus, Titan and possibly Callisto [3]. Interest in the Outer Planet systems currently continues and therefore missions to these destinations have been recommended by both ESA's Voyage 2050 Committee [3] and NASA's 2023-2032 Planetary Science and Astrobiology Decadal Survey [4].

Exploring the potential habitability of the ocean worlds, searching for biosignatures, or studying their environments and interiors requires new missions to have a dedicated science phase, which would typically begin after the corresponding moon tour sequence that brings the spacecraft down from the orbit insertion manoeuvre after the interplanetary transfer to the moon of interest. Once this *pump-down* sequence has been conducted, the desired exploration phase can begin, either by entering into orbit around the moon or by following a pseudo-orbiter strategy. While the former option requires a dedicated manoeuvre, in the latter the spacecraft explores the desired target by means of close flybys which enable to map specific regions of the surface while remaining in orbit around the primary

body (i.e Jupiter or Saturn).

This technique presents several advantages, such as being the least expensive in terms of propellant consumption and thus allowing for greater mass allocation to scientific instrumentation [5], enabling a *store and forward* data transmission approach which allows for higher power instruments usage during the flyby or reducing the radiation dose experienced by the spacecraft due to the flexibility in achieving orbit apoapsis mitigating the effect of the planet's magnetosphere [6]. As a result, this type of trajectory has already been used by Cassini [7] and is planned for the upcoming JUICE [8] and Europa-Clipper [9].

However, for this strategy to provide the desired results a considerable number of well distributed low-altitude flybys have to be performed [10]. Therefore, designing such type of pseudo-orbiter phases requires solving a path-planning problem, where a large set of trajectory possibilities involving resonant and non-resonant transfers is available, as well as dealing with a potentially large number of constraints and competing objectives (eg: high priority regions, science of opportunity events, solar phase angle constraints, maximum eclipse duration, radiation dose, etc). In addition, the problem is further complicated by the difficulty in defining the surfaces/regions of the moon and the criteria to satisfy in order for a certain area to be considered mapped, since the latter depends inherently on instrumentation characteristics which are typically poorly defined during preliminary mission design.

Therefore, it is convenient to conceive the design of a the pseudo-orbiter strategy as a constraint satisfaction problem (CSP) [11], where the aim is to find all the trajectory options that are compliant with the set of mission-driven constraints and, among those, also with an optimal solution with respect to the objective function of interest. Doing so would alleviate the current requirement for substantial a priori knowledge and expertise and provide the mission designer with a great degree of flexibility. To tackle the CSP, an *exhaustive* search algorithm such as breadth-first (BF) or depth-first (DF) should be used, thus ruling out stochastic optimization algorithms since they perform *incomplete* searches [12].

This paper therefore proposes an approach based on the

transcription of the search space into a set of discrete nodes, which are connected by means of moon flybys. Doing so enables to construct the corresponding graph adjacency matrix, as well as to evaluate the surface mapping according to different criteria and constraints. To explore the graph, a breadth-first algorithm is used, and a beam width is implemented to manage the dimensions of the solution set. The results obtained showcase that this enables for a computationally efficient exploration of the search space which provides multiple trajectory options performing a global mapping of the moons, useful for trade-off analysis in preliminary mission design.

II. SEARCH SPACE DEFINITION

To solve the path-planning problem and thus design pseudo-orbiter phases, it is first necessary to define the search space of possible transfers. To that end, the key concept is that of the node, which corresponds to the minimum set of discrete parameters that are required to characterize a planet-centric orbit which has a moon encounter. Since the patched-conic approximation is typically used during preliminary mission design [9] [13], flybys are considered as hyperbolic orbits relative to the moon and the nodes can therefore be characterized in terms of three parameters: the hyperbolic excess velocity v_∞ , the pump angle α and the crank angle k . This therefore enables to define a node as $N = (v_\infty, \alpha, k)$.

An MGA pseudo-orbiter trajectory can then be seen as a sequence of nodes, with the link between a pair of nodes corresponding to a flyby. Since the objective is to ensure subsequent encounters with the same moon, the following same-body ballistic transfers, i.e., without deep space manoeuvres, have been considered:

- *Full resonant* transfers. On such transfers, a ratio of integers exists between the moon and spacecraft orbit periods. The ratio is $N:M$, where N and M are the integer number of moon and spacecraft revolutions, respectively. This implies that the spacecraft encounters the flyby body always at the same position on its orbit after $M \cdot 360$ degrees revolutions. For a given v_∞ and $N:M$ ratio, an infinite number of resonant orbits exist, depending on the value of $k \in [0, 360]$ degrees, which is related to the inclination of the orbit [13]. In this paper, k is discretized according to the maximum bending angle achievable at a specific v_∞ . Note that the pump angle is derived for each pair of v_∞ and resonance ratio.
- *Pseudo-resonant* transfers. On such transfers, the spacecraft encounters the moon on a different position along its orbit, and thus the transfer must be contained on the moon's orbital plane. For a given v_∞ and resonant ratio $N:M$, the full-resonant orbit period is slightly increased ($N:M^+$) or decreased ($N:M^-$) until the flight time to the next encounter matches the one of the flyby body. On $N:M^+$, the spacecraft leaves the moon

inbound (i.e., $k = 0$ degrees) and re-encounters it outbound (i.e., $k = 180$ degrees). The opposite occurs for $N:M^-$ transfers.

- *Back-flip* transfers, also called 180-degree transfers, or π -transfers. On such transfers, the period and eccentricity of the spacecraft orbit match that of the flyby body, and the successive encounter is performed 180 degrees later. It can be shown [13] that, for a given v_∞ , only two orbits are possible for such transfer, depending on the inclination: one prograde orbit, and one retrograde orbit.

Fig 1 shows examples of such transfers for Callisto flybys at $v_\infty = 2.5$ km/s.

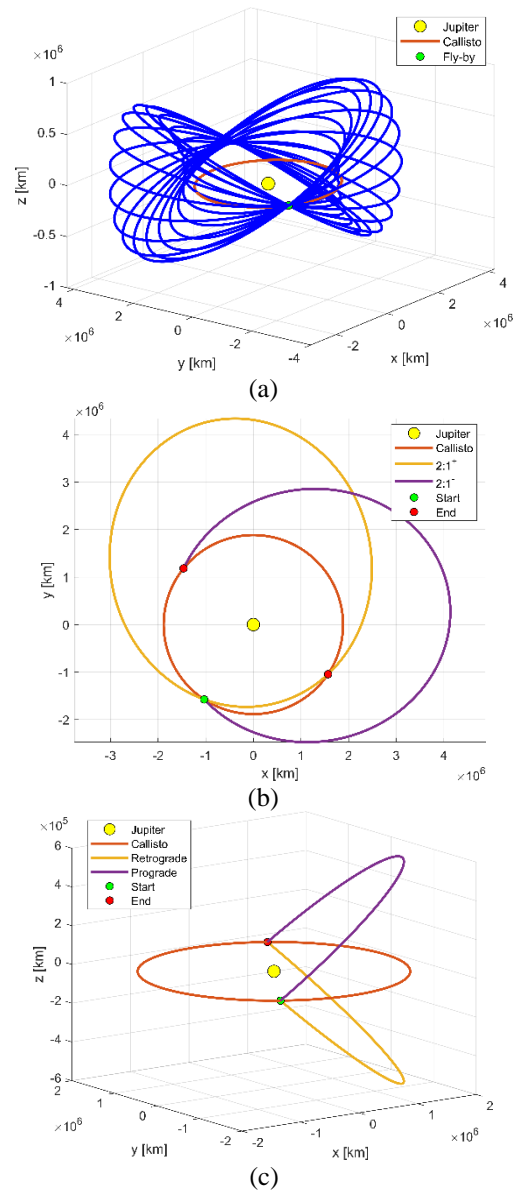


Fig 1: Full-resonant (a), pseudo-resonant (b) and back-flip (c) transfers at Callisto with $v_\infty = 2.5$ km/s.

The search space for pseudo-orbiter trajectories is

therefore composed of a set of nodes, and its structure corresponds to that of a graph. In particular, the graph G is defined by two finite sets V and E [14], where the elements of V are the vertices of the graph and correspond to the nodes representing the aforementioned planet-centric orbits and the elements of E are the edges of the graph and correspond to moon flybys (i.e., the connection between a pair of vertices). Since the change in pump and crank imparted by a flyby is constrained by the maximum bending that can be achieved, it is possible to evaluate all the possible node combinations and to define the corresponding Graph Adjacency Matrix, where the information regarding which flybys (i.e edges) are feasible is contained and constitutes a “database”. Since each feasible edge indicates from which node to which node the spacecraft can transfer, the graph G is *directed*.

When evaluating all the possible transfer combinations it is also possible to obtain and store the associated flyby parameters, such as the latitude and longitude of the flyby periapsis point, the full ground-tracks or the surface area mapped below a certain altitude if an instrument swath is assumed. It is worth noting the construction of the graph adjacency matrix must only be carried out once for each search space discretization, since the exploration is independent from this as will be seen in Section III.

III. EXPLORATION USING A DETERMINISTIC STRATEGY

Exploring the search space and thus building pseudo-orbiter trajectories is achieved by traversing the graph and concatenating nodes to form a sequence. However, to do so an objective or cost function must be associated to each transfer, since the aim is to solve the CSP and to obtain optimal trajectories with respect to the parameters of interest. To that end, one or several *weight functions* W characterizing the cost/performance associated to each flyby (i.e., edge) can be associated to the graph adjacency matrix [14]. Such functions can be, for instance, expressed in terms of time of flight if the transfer cost is being considered, since for the current problem only ballistic transfers are being used. On the other hand, other weight functions could be used to quantify the quality of the flyby, for instance assigning a score depending on the scientific interest of the area above which the spacecraft has flown.

Determining the quality of the flyby or defining the criteria to satisfy for a certain moon to be considered mapped is not straightforward. One approach was proposed in the 6th edition of the Global Trajectory Optimization Competition (GTOC), where the moon surface was divided into 32 polygons, each of which had

an associated score. A polygon was considered mapped if the flyby periapsis location was contained inside its bounds and if the altitude was between 50 and 2000 km. Other approaches, such as those found in mission analysis studies for Laplace/JUICE [5] and Europa Clipper [9] have divided the surface into rectangles defined in terms of latitude and longitude, with these areas being considered mapped whenever the ground track points fell inside and respected certain altitudes limits. Examples of these two options are shown in Fig 2, where it is possible to see the different results that would be achieved, since the GTOC 6 approach would consider one sector mapped while the other strategy would result in three. For this paper, the approach selected has been the latter, with the moon surface being divided into rectangular sectors and mapping of the sector being considered achieved if at least one point of the ground track is inside and respects a maximum altitude constrain. Consequently, a global mapping of the moon is fulfilled when all the sectors into which the surface has been divided are mapped.

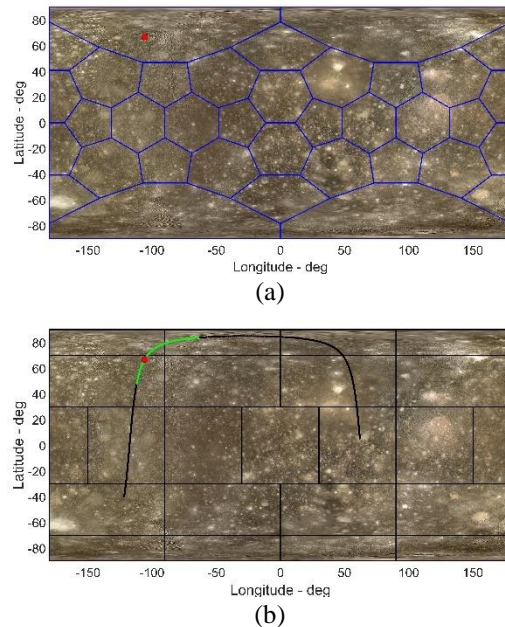


Fig 2: Examples of mapping definitions using (a) the GTOC 6 approach (b) the ground-tracks and rectangles, for a transfer from a 3:1 resonance at 0° crank to a 2:1 resonance with crank 61.71° at Callisto with $v_{\infty} = 2.1$ km/s. The red points correspond to the periapsis of the flyby hyperbola, while green are ground track points below the maximum altitude constraint, established at 300km, and black are ground track points above this altitude.

With the graph adjacency and its associated weight functions defined, the CSP can then be solved by performing an exhaustive search, which has the objective of achieving a global mapping of the moon. To that end, a breadth-first algorithm has been implemented, so that the exploration of the graph starts from a user-selected node and then branches are expanded one level at a time. After each expansion, the

existing solutions can be ranked according to different criteria and the process is repeated until a global mapping is achieved. The depth of the tree, that is, how many levels to expand, can be controlled by imposing a maximum time of flight or a maximum number of flybys, thus limiting the computational effort and enabling to impose constraints in these two parameters to eliminate pseudo-orbiter trajectories not respecting the associated bounds. Furthermore, since this is in essence an NP-hard combinatorial problem [15], a beam width can be implemented to manage the dimensions of the tree and thus control the computational time required, such that at each level only the solutions ranking inside the user-defined beam width are retained for further expansion. Fig 3 presents a schematic representation of the process.

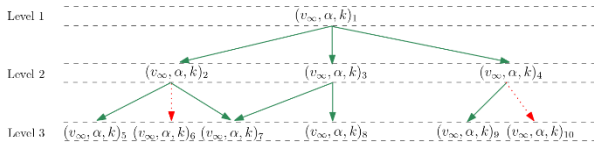


Fig 3: Schematic representation of the breadth-first exploration of the graph and how a beam width (of size 5 in this example) is applied. Green arrows represent the retained feasible paths, red arrows are paths which are pruned and lack of arrows showcases unfeasible flybys between those nodes.

The exploration of the search space and the resulting pseudo-orbiter trajectories that are obtained have the important feature of being time independent. Consequently, this approach is epoch-free and generates a large database of tours which involve the same nodes and transfers independently of the date at which the pseudo-orbiter phase starts. From this set of solutions, it is then possible to select for further analysis those tours which appear more promising, to process and include time-dependent characteristics that may be of interest, such as for instance the illumination conditions.

IV. RESULTS

To assess the efficiency and effectiveness of the proposed methodology, the search for pseudo-orbiter tours has been conducted for Callisto and Enceladus. This moon's choice was made with two objectives: firstly, to reference the results being obtained with those from the literature available for Callisto [5] and Enceladus [16]; secondly, to showcase the universality of the tool and how it can be used to obtain these types of trajectories even for minor moon's such as Enceladus, where the bending achievable with each flyby is considerably smaller than the one available with larger bodies.

To that end, several heuristics and pruning criteria are used in the global search. These are:

- During a flyby, the altitude to allow mapping a sector

is set to 300 km, similarly to one of the requirements in [5], while the minimum altitude for periapsis passage is $h_{map} \geq 50$ km.

- The global search for tours is ended at a depth of 20 (i.e., 21 flybys including the first encounter).
- The maximum number of solutions kept at each expansion level, the beam width, is set to 100,000.
- To construct the database of nodes as in Section II, the list of resonances employed for each moon was retrieved from [5] [16] and is found in Table 1.

Moon	Resonances
Callisto	1:1, 2:1, 3:1, 4:1, 3:2, 2:3
Enceladus	1:1, 7:6, 20:17, 15:13, 8:7, 17:15, 9:8, 19:17, 10:9, 21:19, 11:10, 12:11, 13:12, 14:13, 15:14, 16:15, 19:18, 24:23, 17:16, 21:20, 13:11, 22:19, 15:13, 25:22, 18:17

Table 1: List of resonances being considered for each moon.

The analysis also intends to find trajectory options which not only achieve a global mapping but that also satisfy typical scientific requirements, such as for example the necessity to have polar and equatorial flybys of the moon [5]. Therefore, the following sections will present results for three scenarios:

- A simple global mapping of the moon, achieved by flying over all the sectors and respecting the aforementioned altitude values.
- A global mapping which includes at least one polar flyby, defined as a flyby with at least one point at 90° latitude.
- A global mapping including at least one polar and one equatorial flyby, with the latter being a flyby in which all ground track points fall in the $[-5^\circ, +5^\circ]$ latitude range.

Pseudo-orbiter options for Callisto at 2.1 km/s

For Callisto, the search is assumed to start from an initial Jupiter equatorial orbit crossing its orbit, defined by the node $(v_\infty, \alpha, k) = (2.1 \frac{km}{s}, 27.6 \text{ deg}, 0 \text{ deg})$. This corresponds to an orbit with $r_a = 5976356.26$ km, $r_p = 1857807.76$ km and zero inclination, encountering the moon inbound. As explained, this node was selected to have similar initial conditions to those in available literature [5]. The generation of the graph adjacency matrix (the database from Section II) required 56.6 seconds, while the full exploration 1210.78 seconds using an Intel Core i7-12800H processor.

Results are summarized in Fig 4, representing the minimum time for globally mapping Callisto with respect to the number of flybys with the moon.

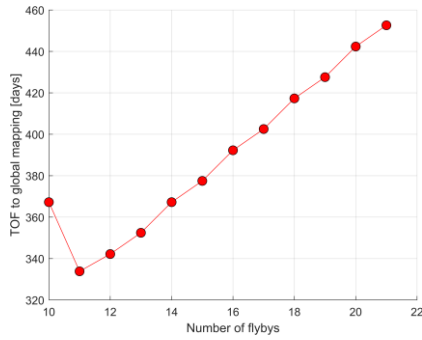


Fig 4: Time of flight (TOF) for global mapping with respect to the number of flybys.

Interestingly, the minimum number of flybys to achieve global mapping is 10, but this does not correspond to the minimum duration. This is mainly because high resonant ratios (i.e., 3:1 and 3:2) are used in most of the legs. The minimum duration to globally map the moon is achieved with 11 flybys and lasts for 333.85 days. This option is represented in Fig 5. Specifically, Fig 5a shows the ground-tracks during each flyby, where green colour is used to highlight the opportunities for mapping a sector according to the constraint $h_{map} \geq 50$ km. Notably, one flyby has a pure equatorial ground-track, but no mapping is performed as the constraint $h_{map} < 300$ km is not satisfied. Fig 5b represents the corresponding trajectory around Jupiter. As can be seen, only full-resonant transfers are sufficient to globally map the moon, and the resonances used are 2:1, 3:1, 3:2 and 1:1.

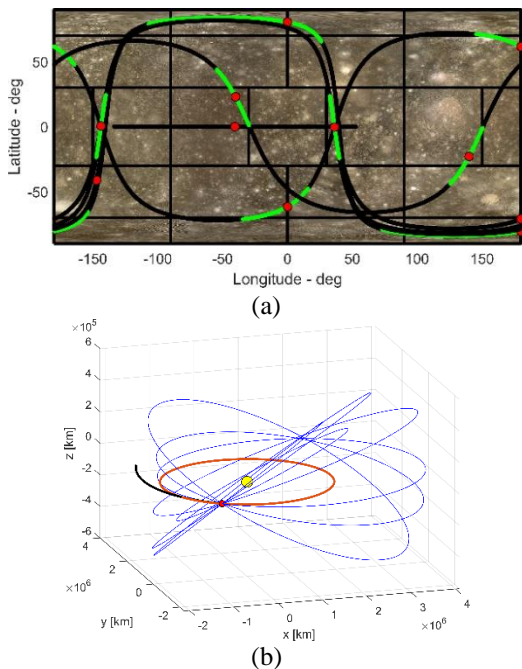


Fig 5: Ground-tracks (a) and trajectory (b) for the minimum-time-of-flight solution to globally map Callisto.

One crucial advantage of the search described in section

III is that multiple and different tours are given in the final solutions' set. In this way, multiple trajectory options are provided in preliminary mission design, answering the need for tours' options accounting for different constraints and/or mission requirements. For example, one might require that at least one tour passes over the polar regions, performing a flyby with 90-degrees latitude. Fig 6.a and Fig 6.b show ground-tracks during flybys and trajectory of such option, respectively. The minimum time to globally map the moon with the given constraint is 367.23 days with 10 flybys. Again, only full-resonant transfers are employed, with ratios 2:1, 3:1, 3:2 and 1:1.

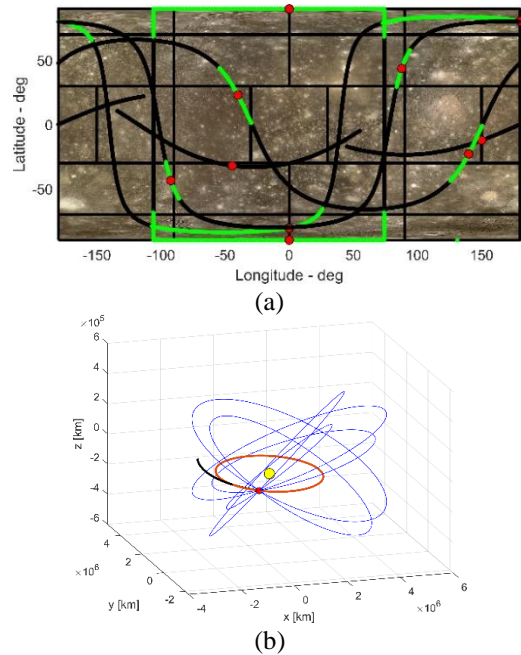
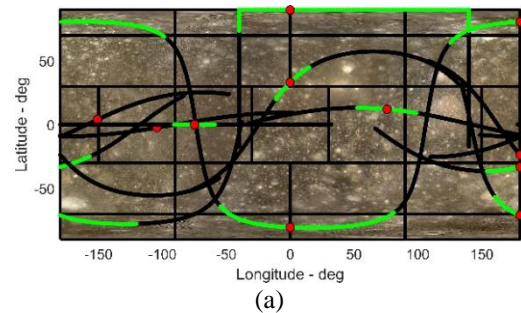


Fig 6: Ground-tracks (a) and trajectory (b) for the minimum-time-of-flight solution to globally map Callisto enforcing at least one polar flyby.

Finally, if one adds the additional requirement of having at least one flyby passing over the equator, one has the solution represented in Fig 7.a (ground-tracks) and Fig 7.b (trajectory). The minimum time to globally map the moon with this additional constraint is 370.47 days, with 11 flybys. This specific tour requires both full-resonant and pseudo-resonant transfers, with ratios 2:1, 3:1 and 1:1 being used.



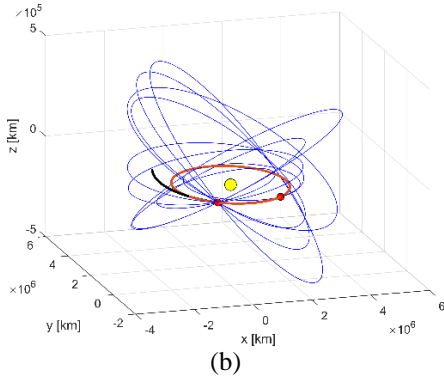


Fig 7: Ground-tracks (a) and trajectory (b) for the minimum-time-of-flight solution to globally map Callisto enforcing at least one polar and one equatorial flyby.

Enceladus pseudo-orbiter at 0.7 km/s

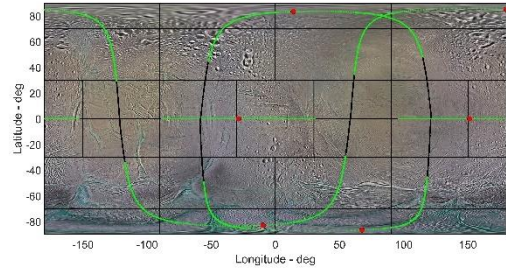
The search is assumed to start from a similar initial condition as that found in [16], and which is defined by the node $(v_{\infty}, \alpha, k) = (0.7 \frac{km}{s}, 26.06 \text{ deg}, 0 \text{ deg})$. This corresponds to a 20:17 resonant orbit with Enceladus, with zero inclination. The results obtained for this exploration are presented in Table 2, where it is possible to see that hundredths of thousands of solutions were obtained with a computational time of 10.7 minutes to build the graph adjacency matrix and of 16.9 minutes to carry out the search, using an Intel Core i7-12800H processor. The effect of a smaller bending can be appreciated in the computation time, which is greater compared to the results obtained previously for Callisto due to the refined discretization which leads to a larger number of nodes.

N° of Flybys	N° of solutions	Min. TOF to global mapping
6	100	57.56
7	5332	67.02
8	76919	76.62
9	201586	86.21
10	206064	95.80
11	239801	105.40
12	243328	114.99
13	216710	124.59
14	212359	134.18
15	206333	143.78
16	193610	153.37
17	177367	162.96
18	162854	172.56
19	152526	182.15
20	140839	191.74

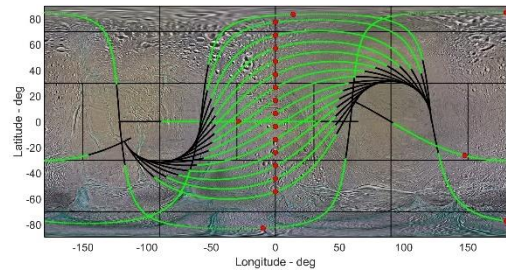
Table 2: Number of unique solutions obtained for the mapping of Enceladus with $v_{\infty} = 0.7 \text{ km/s}$.

The large set of trajectories that are obtained provides great flexibility, since the mission designer can search through the solutions to find options satisfying mission-specific requirements. Similarly to the analysis carried

out for Callisto, Fig 8 show the ground-tracks of the trajectories involving 6 and 20 flybys and minimum time of flight which achieve a global mapping of the moon according to the previously explained criteria. Both solutions use the 20:17, 7:6 and 13:11 resonances, but the second trajectory has a TOF of 191.74 days because it includes a crank-over the top (COT) sequence using the 7:6 resonance.



(a)



(b)

Fig 8: Ground-tracks for the two solutions involving minimum TOF to achieve Enceladus global mapping at $v_{\infty} = 0.7 \text{ km/s}$ with (a) 6 flybys (b) 20 flybys, with a COT sequence using the 7:6 resonance.

If the objective is to have at least one polar and one equatorial flyby, then a quick search through the catalogue of solutions yields numerous options, as shown in Table 3. The solution with minimum TOF and involving 6 flybys is presented in Fig 9, where in (b) one can see that it also employs a pseudo-resonant transfer that enables to change the longitude of the encounter.

N° of Flybys	N° of solutions
6	8
7	217
8	3782
9	4895
10	5358
11	3859
12	7174

Table 3: Number of solutions including at least one polar and one equatorial passage.

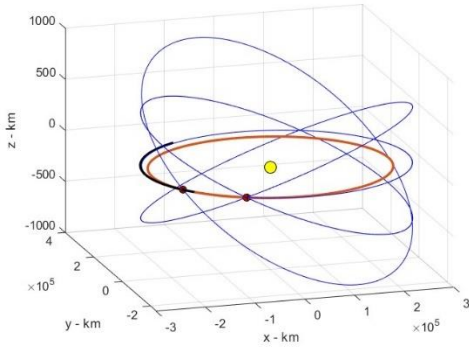
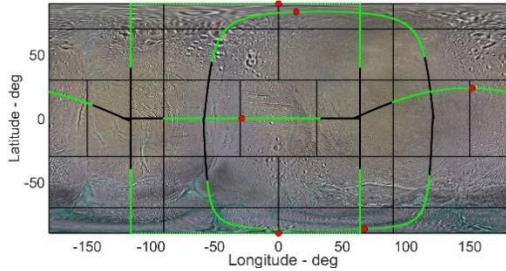


Fig 9: Ground-tracks (a) and trajectory (b) for the minimum-time-of-flight solution to globally map Enceladus with at least one polar and one equatorial flyby.

Enceladus pseudo-orbiter at 1.5 km/s

Designing pseudo-orbiter trajectories around minor moon's which have a low gravitational parameter is further complicated as the hyperbolic excess velocity increases, since this leads to smaller bending angles being achievable. For instance, for $v_{\infty} = 1.5$ km/s the maximum bending angle is 1.31° , which corresponds to a 77% decrease with respect to that available at $v_{\infty} = 0.7$ km/s. Consequently, it is necessary to use a more refined discretization of the nodes, which causes the computational time of the graph adjacency matrix to be 22.48 minutes, more than double the time required for the case at $v_{\infty} = 0.7$ km/s. The exploration of the graph is carried out from the starting node $(v_{\infty}, \alpha, k) = (1.5 \frac{km}{s}, 68.11^{\circ}, 0^{\circ})$, which corresponds to a 20:17 resonance with Enceladus, as was done before for the analysis at $v_{\infty} = 0.7$ km/s. The results obtained are presented in Table 4, where it is seen that the proposed approach is capable of still finding hundredths of thousands of solutions. It is worth noting that the minimum number of flybys to map the moon has increased, passing from 6 flybys to 8, and that the fastest global mapping is achieved with 9 or 10 passages, since the resonance ratios used are smaller.

N° of Flybys	N° of solutions	Min. TOF to global mapping
8	148	121.57
9	7050	113.75
10	46956	113.75

11	63710	123.34
12	89425	132.93
13	111271	142.53
14	118504	152.12
15	118504	171.31
16	127176	180.90
17	125060	190.49
18	123542	200.09
19	122092	209.68
20	121358	219.28

Table 4: Number of unique solutions obtained for the mapping of Enceladus with $v_{\infty} = 1.5$ km/s.

Two solutions achieving the global mapping of the moon in the minimum TOF (113.75 days) are presented in Fig 10, one using 9 flybys with the 20:17 and 7:6 resonances, and the other employing 10 flybys with 20:17, 7:6 and 13:11 resonances. Compared to the results in Fig 8 and Fig 9, it is possible to appreciate that the ground tracks respecting the 300km altitude for each flyby are smaller in terms of latitude/longitude extension. In addition, several sectors in the $[-20^{\circ}, +20^{\circ}]$ latitude range are considered mapped even though very few points of the ground track fall inside, thus showcasing the limitations of the mapping definition being used and that establishing a criteria to consider a surface mapped is not straightforward.

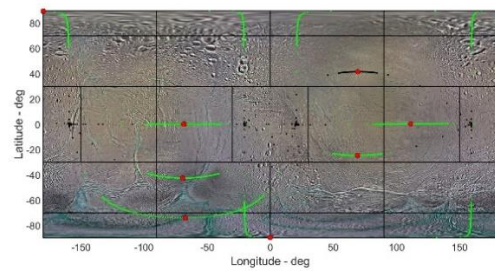
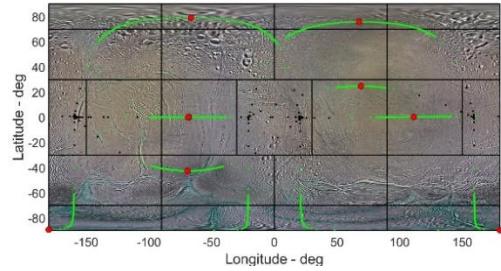


Fig 10: Ground tracks for the trajectories globally mapping Enceladus at $v_{\infty} = 1.5$ km/s with (a) 9 flybys (b) 10 flybys.

V. CONCLUSIONS

To explore the moons of the Outer Planets one strategy is to carry out a pseudo-orbiter phase. To design these trajectories, a path-planning problem must be solved, where numerous options involving resonant and non-resonant transfers exist.

To tackle this problem, this paper has proposed a two-step automated approach. Firstly, the search space is defined as a set of time-independent nodes, expressed in terms of (v_{∞}, α, k) , and a graph adjacency matrix is constructed after evaluating all the possible combinations. The resulting graph is explored by means of a deterministic breadth-first algorithm, where the user selects the initial node and branches are expanded one level at a time. At each expansion, existing solutions are ranked according to the criteria of interest and the process is repeated until a global mapping of the moon is achieved, with a beam width of 100,000 being implemented at each level to manage the tree dimensions and thus control computational time.

The advantages of these approach are threefold: firstly, it completely decouples the construction of the search space from its exploration, and thus the graph adjacency matrix only has to be obtained once; secondly, the exploration solves the associated constrain satisfaction problem (CSP) and is epoch-independent, yielding a catalogue of solutions including hundredths of thousands of pseudo-orbiter sequences, thus providing the mission designer with a large set of options; thirdly, the computation time is maintained in the order of tens of minutes, ideal for rapid analyses during preliminary mission design. Results are presented for Callisto and Enceladus, showcasing the usefulness of the approach.

VI. REFERENCES

- [1] B. Smith, L. Soderblom, R. Beebe, J. Boyce, G. Briggs, M. Carr, S. Collins, A. Cook, G. Danielson, M. Davies, G. Hunt, A. Ingersoll, T. Johnson, H. Masursky, J. McCauley, D. Morrison, T. Owen, C. Sagan, E. Shoemaker, R. Strom, V. Suomi and J. Veverka, "The Galilean Satellites and Jupiter: Voyager 2 Imaging Science Results," *Science*, vol. 206, no. 4421, pp. 927-950, 1979.
- [2] S. M. Krimigis, J. F. Carbary, E. P. Keath, T. P. Armstrong, L. J. Lanzerotti et G. Gloeckler, «General characteristics of hot plasma and energetic particles in the Saturnian magnetosphere: Results from the Voyager spacecraft,» *Journal of Geophysical Research: Space Physics*, vol. 88, n° %1A11, pp. 8871-8892, 1983.
- [3] L. J. Tacconi, C. S. Arridge, A. Buonanno, M. Cruise, O. Grasset, A. Helmi, L. Iess, E. Komatsu, J. Leconte, J. Leenaarts, J. Martin-Pintado, R. Nakamura et D. Watson, «Voyage 2050: Final recommendations from the Voyage 2050 Senior Committee,» 2021.
- [4] National Academies of Sciences, Engineering and Medicine, *Origins, Worlds, and Life: A Decadal Strategy for Planetary Science and Astrobiology 2023-2032*, Washington DC: The National Academies Press, 2022.
- [5] A. Boutonnet, J. Schoenmaekers et P. D. Pascale, «Laplace: an update of the science phases around Callisto and Ganymede,» chez *AAS/AIAA Space Flight Mechanics Meeting*, San Diego, US, 2010.
- [6] B. Buffington, N. Strange et S. Campagnola, «Global Moon Coverage via Hyperbolic Flybys,» chez *23rd International Symposium on Space Flight Dynamics*, Pasadena, US, 2012.
- [7] A. A. Wolf et J. C. Smith, «Design of the Cassini tour trajectory in the Saturnian system,» *Control Engineering Practice*, vol. 3, n° %111, pp. 1611-1619, 1995.
- [8] G. Sarri, O. Witasse et C. Cavel, «The JUICE Mission to Jupiter and its Icy Moons,» chez *9th European Conference for Aeronautics and Space Sciences*, Lille, France, 2022.
- [9] S. Campagnola, B. Buffington, T. Lam, A. E. Petropoulos et E. Pellegrini, «Tour Design Techniques for the Europa Clipper Mission,» chez *69th International Astronautical Congress*, Bremen, Germany, 2018.
- [10] E. M. Alessi et P. Pergola, «Two options for the Callisto's exploration,» *Acta Astronautica*, vol. 72, pp. 185-197, 2012.
- [11] S. C. Brailsford, C. N. Potts et B. M. Smith, «Constraint satisfaction problems: Algorithms and applications,» *European Journal of Operational Research*, vol. 119, n° %13, pp. 557-581, 1999.
- [12] S. Prestwich, «The Relation Between Complete and Incomplete Search,» chez *Hybrid Metaheuristics: An Emerging Approach to Optimization*, Springer Berlin Heidelberg, 2008, pp. 63-83.
- [13] N. Strange, «Analytical methods for gravity-assist tour design,» PhD Thesis, Purdue University, 2016.
- [14] J. M. Harris, J. L. Hirst et M. J. Mosinghoff, *Combinatorics and Graph Theory*, Springer, 2008.
- [15] T. Cormen, C. Leiserson, R. Rivest et C. Stein, *Introduction to Algorithms*, The MIT Press, 2009.
- [16] S. Campagnola, N. J. Strange et R. Russell, «A fast tour design method using non-tangent v-infinity,» *Celestial Mechanics and Dynamical Astronomy*, vol. 108, pp. 165-186, 2010.
- [17] A. E. Petropoulos, «Problem Description for the 6th Global Trajectory Optimisation Competition,» 10 09 2012. [En ligne]. Available: https://sophia.estec.esa.int/gtoc_portal/wp-content/uploads/2012/11/gtoc6_problem_stmt-2.pdf. [Accès le 04 04 2024].